



An Updated Small Magellanic Cloud and Magellanic Bridge Catalog of Star Clusters, Associations, and Related Objects

Eduardo Bica¹, Pieter Westera² , Leandro de O. Kerber³ , Bruno Dias^{4,5} , Francisco Maia^{6,7} , João F. C. Santos Jr.⁸ ,
Beatriz Barbuy⁷, and Raphael A. P. Oliveira⁷ 

¹ Universidade Federal do Rio Grande do Sul, Instituto de Física, Av. Bento Gonçalves 9500, 91501-970, Porto Alegre, Brazil

² Universidade Federal do ABC, Centro de Ciências Naturais e Humanas, Avenida dos Estados, 5001, 09210-580, Santo André, Brazil; pieter.westera@ufabc.edu.br

³ Universidade Estadual de Santa Cruz, Depto. de Ciências Exatas e Tecnológicas, Rodovia Jorge Amado km 16, 45662-900, Ilhéus, Brazil

⁴ Universidad Andrés Bello, Facultad de Ciencias Exactas, Departamento de Física, Av. Fernandez Concha 700, Las Condes, Santiago, Chile

⁵ Instituto Milenio de Astrofísica, Av. Vicuña Mackenna 4860, Macul, 7820436 Santiago, Chile

⁶ Universidade Federal do Rio de Janeiro, Instituto de Física, Av. Athos da Silveira Ramos, 149, 21941-972, Rio de Janeiro, Brazil

⁷ Universidade de São Paulo, Instituto de Astronomia, Geofísica e Ciências Atmosféricas, Rua do Matão 1226, 05508-090, São Paulo, Brazil

⁸ Universidade Federal de Minas Gerais, Departamento de Física, ICEx, Av. Antonio Carlos 6627, 31270-901 Belo Horizonte, MG, Brazil

Received 2019 April 4; revised 2019 December 18; accepted 2019 December 19; published 2020 February 3

Abstract

We present a catalog of star clusters, associations, and related extended objects in the Small Magellanic Cloud (SMC) and the Magellanic Bridge with 2741 entries, a factor 2 more than a previous version from a decade ago. Literature data up until 2018 December are included. The identification of star clusters was carried out with digital atlases in various bands currently available in the Digitized Sky Survey and the Machine Automatique à Mésurer pour l’Astronomie. imaging surveys. In particular, we cross-identified recent cluster samples from the Visible and Infrared Survey Telescope for Astronomy near-infrared YJK_s survey of the Magellanic System, Optical Gravitational Lensing Experiment IV, and Survey of the MAgellanic Stellar History surveys, confirming new clusters and pointing out equivalencies. A major contribution of the present catalog consists of the accurate central positions for clusters and small associations, including a new sample of 45 clusters or candidates in the SMC and 19 in the Magellanic Bridge, as well as a compilation of the most reliable age and metallicity values from the literature. A general catalog must also deal with the recent discoveries of 27 faint and ultra-faint star clusters and galaxies projected on the far surroundings of the Clouds, most of them from the Dark Energy Survey. The information on these objects has been complemented with photometric, spectroscopic, and kinematical follow-up data from the literature. The underluminous galaxies around the Magellanic System, still very few as compared to the predictions from Λ Cold Dark Matter simulations, can bring constraints to galaxy formation and hierarchical evolution. Furthermore, we provide diagnostics, when possible, of the nature of the ultra-faint clusters, searching for borders of the Magellanic System extensions into the Milky Way gravitational potential.

Unified Astronomy Thesaurus concepts: Celestial objects catalogs (212); Small Magellanic Cloud (1468); Star clusters (1567); Galaxy interactions (600)

Supporting material: machine-readable table

1. Introduction

Star clusters, associations, and the field stellar population in the Magellanic Clouds (MCs), together with their tidal Magellanic Bridge (MB), are essential components to understand the past and future evolutionary stages of the system as a whole. The Clouds, together with the Milky Way, act as a nearby theater of galaxy interactions (Bekki 2012). These different components play a key role in terms of age distributions (Glatt et al. 2010), age–metallicity relations (AMRs; Cignoni et al. 2013), dynamics (Subramanian et al. 2017; Kallivayalil et al. 2018), cluster distribution (Bica et al. 2008a, hereafter Paper I), cluster structure (Maia et al. 2014), and galaxy structure (Crowl et al. 2001), just to mention a few subjects and studies about them.

The study of the Small Magellanic Cloud (SMC) clusters basically starts with the lists by Kron (1956) and Lindsay (1958), with 69 and 116 clusters respectively, where the Kron’s objects were included in Lindsay’s list. Deeper photographic plates, taken by Hodge (1986, hereafter H86), provided 213 new relatively faint clusters, including small associations. Associations in the SMC were cataloged for instance by Hodge (1985) and Bica & Schmitt (1995, hereafter BS95).

Some MB clusters have recently been photometrically studied resulting, as a rule, in young ages (Bica et al. 2015, hereafter BS15; Piatti et al. 2015). Associations in the MB are extended with low stellar density (Demers & Battinelli 1998, and references therein). The field population has also constrained the tidal formation and evolution of the MB (Belokurov et al. 2017; Carrera et al. 2017), whereas the determination of the SMC star formation history with the Visible and Infrared Survey Telescope for Astronomy (VISTA) near-infrared YJK_s survey of the Magellanic System (VMC) provided an SMC tomography (Rubele et al. 2015).

BS95 were the first to put together and cross-identify clusters, associations and related objects (hereafter CAROs) in the SMC and MB. In BS95, 284 new clusters and associations were also reported. A few years later, Bica & Dutra (2000) updated the SMC/MB census. In Paper I, the SMC and MB were presented together with the Large Magellanic Cloud (LMC) CAROs. Paper I listed 635 star clusters, 385 emissionless associations, and 316 associations related to emission nebulae (including supernova remnants, hereafter SNRs), totaling 1336 entries in the SMC and MB, and 7175 CAROs in the LMC.

Table 1
Literature Sources Used for the Cross-identification

Reference (1)	Main Contribution(s) (2)	Designations (3)
Westerlund (1964)	SMC wing clusters	NGC 602-A, NGC 602-B
Kunkel (1980)	Association in the Bridge	Kunkel's Association (KA)
Chiosi et al. (2006)	Three clusters projected on or related to SNRs	CVH
Paper I	Departure catalog	Paper I and references therein
Paper I	Tidal dwarf galaxies in the Bridge	BS I, BS II, BS III
Cignoni et al. (2009)	SMC wing cluster	NGC 602-B2
Schmeja et al. (2009)	Small clusters in NGC 346 with <i>HST</i>	SGK
Badenes et al. (2010)	SMC SNRs, multiwavelength	SNR
Piatti et al. (2016)	Central SMC IR clusters with VMC in the near-IR	VMC
Piatti (2017)	SMC outskirts and main body with SMASH	Piatti or SMASH
Sitek et al. (2017)	SMC outskirts and Bridge with OGLE-IV	OGLEs, OGLB ^a
Bitsakis et al. (2018)	1175 new objects (mostly associations) in the near-UV and IR	BUS, BIS, BMS
Present paper	64 new SMC/Bridge clusters with Aladin	SBica, BBica
Present paper	Updated SMC/Bridge catalog with 2741 entries	See present and previous versions

Note.

^a OGLE clusters have two databases: (i) the first cluster series was given the acronym SOGLE for SMC clusters (Paper I). (ii) Concerning the recent OGLE-IV cluster series (Sitek et al. 2017), we employ the acronyms OGLEs and OGLB for their SMC and Bridge clusters, respectively, for the sake of simplicity and space. Note that SBica 9 and 34 turned out to be duplications of BS13 and BS76, respectively.

The study of CAROs in the Clouds depends on technological advances, such as high spatial resolution and/or different spectral domains to probe their contents deeper. Ten years have elapsed since the last census (Paper I), and interesting new clusters and associations have been identified in this period. Besides, new surveys with larger telescope apertures and resolving power took place, as well as ultraviolet (UV) and infrared (IR) surveys complementing the optical ones (e.g., Piatti 2017; Sitek et al. 2017; Bitsakis et al. 2018). Finally, the far surroundings of the Clouds were surveyed with the Dark Energy Survey (DES; e.g., Drlica-Wagner et al. 2015) and complemented with deep follow-up studies (e.g., Conn et al. 2018). They produced a collection of faint or ultra-faint stellar systems that challenge our current understanding of the formation and hierarchical evolution of galaxies (e.g., Dooley et al. 2017). On the other hand, these systems are establishing new landmarks for ultra-faint clusters formed in the Clouds and kept captive, or dispersed into the Milky Way (MW) potential, as compiled and discussed in the present paper. We also point out that nowadays a general catalog of the SMC/MB (and as perspective the LMC) must include the stellar clusters that, projected on the celestial sphere, seem extremely far from the MC barycenter, therefore constituting an Extended Magellanic System (EMS), in order to better constrain its boundaries.

The new deep photometric survey, Visible Soar photometry of star Clusters in tApii and Coxi HuguA⁹ (VISCACHA; Maia et al. 2019), is using adaptive optics technology to complement the current and past large surveys on the Magellanic Clouds. More specifically, VISCACHA aims at observing the crowded regions of star clusters to get a complete census of their properties. An updated catalog of CAROs in the Magellanic Cloud System will allow a good target selection and observation efficiency.

The aim of the present study is to collect the published information about the CAROs in the last decade and to search for new clusters. One of us (E. B.) inspected Hodge's faint clusters (Hodge 1986) and found new similar objects (SBica in

the SMC and BBica in the Bridge) by analyzing *J* (blue) SMC plates from the UK Schmidt Telescope (Siding Springs, Australia), scanned with the Machine Automatique à Mésurer pour l'Astronomie (MAMA). The latter are often referred to as the MAMA/SERC (Science and Engineering Research Council) plates. The *BRI* combined images from the Digitized Sky Survey (DSS) atlas were also analyzed. We end up with an updated general catalog of the SMC and MB clusters.

In Section 2 we present the observational material and the cross-identification procedures employed. We discuss the studies in the present catalog, together with the new discoveries. In Section 3 we cross-identify objects from previous studies with the ones from the recent SMC objects catalog by Bitsakis et al. (2018). We argue that most of them are associations rather than clusters, by comparison with the previous literature of associations in the Clouds. In Section 4 we explore the new catalog. In Section 5 we present a compilation of ages and metallicities of the catalog objects, and analyze them. In Section 6 we address the small stellar systems that, projected on the celestial sphere, seem far from the LMC and SMC, in view of characterizing an EMS. Finally, in Section 7 concluding remarks are given.

2. New Clusters, Associations, and Candidates

The studies on new SMC and Bridge clusters in the last decade are listed in Table 1, along with three studies prior to Paper I. Column 1 lists the references, column 2 explains the contents, and column 3 gives designations or additional information. These designations are used to list the different object identifications in our new catalog, given in Table 2. In Table 2 we provide data not included in Paper I, as well as some corrections: (i) SMC SNRs in the MC *Chandra* Catalog¹⁰; (ii) the acronym GHK (Paper I) was corrected to GQH (Gouliermis et al. 2007); and (iii) mistakes in Paper I concerning RZ designations (Rafelski & Zaritsky 2005) were corrected.

⁹ <http://www.astro.iag.usp.br/~viscacha/>

¹⁰ https://hea-www.harvard.edu/ChandraSNR/snrcat_lmc.html

Table 2
The General SMC/Bridge Catalog(1)

Designations	J2000 R.A. (hh:mm:ss.s)	J2000 Decl. (Deg:':")	Type(2)	$D(3)$ (')	$d(4)$ (')	Cl.(5)	log(Age)	[M/H]	ref1(6) ^a	ref2(7) ^b	Comments(8)
AM 3,ESO28SC4,OGLS 315	23:48:59.3	-72:56:46	C	0.90	0.90	U	9.72	-0.98	PGC+14, DKB+14	DKB+16	
L1,ESO28SC8,OGLS 313	0:03:54.6	-73:28:16	C	4.60	4.60	U	9.88	-1.04	GGSO8, DKB+16	PGC+15	Globular cluster ?
L2,OGLS 312,OGLS 328	0:12:56.9	-73:29:28	C	1.20	1.20	U	9.6	-1.58	DKB+14	DKB+16	
OGLS 264	0:18:22.1	-71:27:02	C	0.60	0.60	U			
L3,ESO28SC13,OGLS 323,OGLS 327	0:18:25.2	-74:19:05	C	1.00	1.00	U	8.99	-0.65	PGC+14, DKB+14	DKB+16	
...

Notes. (1) Only the first five entries are listed here; the full table is available in electronic format. The marked columns correspond to: (2) type of object as defined in Table 3; (3) major angular size; (4) minor angular size; (5) class of correlation with the BGB+18 catalog; (6) references for age; (7) references for metallicity; and (8) comments and hierarchical relation to other catalog objects (see the text).

^a From newest to oldest, the references for the ages stand for: Bitsakis et al. (2018, BGB+18); Conn et al. (2018, CJK+18); Dias et al. (2016, DKB+16); Piatti et al. (2016, PIR+16); Bica et al. (2015, BSB+15); Palma et al. (2015, PCG+15); Piatti et al. (2015, PdGR+15); Dias et al. (2014, DKB+14); Maia et al. (2014, MPS14); Parisi et al. (2014, PGC+14); Piatti (2014, P14); Piatti & Bica (2012, PB12); Glatt et al. (2010, GGK10); Bica et al. (2008b, BSS08); Glatt et al. (2008, GGG+08); Glatt et al. (2008, GGS+08); Schmalzl et al. (2008, SGD+08); Sabbi et al. (2007, SSN+07); Rochau et al. (2007, RGB+07); Chiosi et al. (2006, CVH+06); Piatti et al. (2005a, PSC+05); Rafelski & Zaritsky (2005, RZ05); Carlson et al. (2007, CSS+07); Pietrzynski & Udalski (1999, PU99); Girardi et al. (1995, GCB+95); Santos et al. (1995, SBC+95); Grondin et al. (1992, GDK92); Demers et al. (1991, DGI+91); Grondin et al. (1990, GDK+90); and van den Bergh (1981, vdB81).

^b For the metallicities, besides the aforementioned references, we adopted: Perren et al. (2017, PPV17); Parisi et al. (2015, PGC+15); Piatti (2012, P12); Piatti (2011a, P11a); Piatti (2011b, P11b); Piatti et al. (2011, PCB+11); Dias et al. (2010, DCB+10); González Delgado & Cid Fernandes (2010, GDC10); Rubele et al. (2010, RKG10); Parisi et al. (2009, PGG+09); Piatti et al. (2007, PSG+07); Piatti et al. (2005b, PSG+05); Piatti et al. (2001, PSC+01); Crowl et al. (2001, CSP+01); Dolphin et al. (2001, DWH+01); Alves & Sarajedini (1999, AS99); da Costa (1999, D99); Hill (1999, H99); de Freitas Pacheco et al. (1998, dFPBI98); da Costa & Hatzidimitriou (1998, DH98); Mighell et al. (1998, MSF98); Alcaino et al. (1996, ALA+96); Mould et al. (1992, MJdC92); Seggewiss & Richtler (1989, SR89); Bica et al. (1986, BDP86) Rich et al. (1984, RdCM84); and Zinn & West (1984, ZW84).

(This table is available in its entirety in machine-readable form.)

Table 3
Updated Census of the SMC and Bridge Extended Objects by Object Class and Correlation with the BGB+18 Catalog

Object Class (1)	Characteristics (2)	Description (3)	I (4)	N (5)	E (6)	U (7)	R (8)	Total (9)
C	Star cluster	Resolved star cluster	0	1	58	529	38	626
CA	Poor cluster transition to small association	Structure looser than clusters	0	0	10	133	13	156
A	Association	...	960	207	21	210	9	1407
AC	Small association, looser than clusters	Association character dominates	0	1	3	62	2	68
CC	Cluster candidate	Nonresolved cluster	0	0	0	39	2	41
NC	Cluster in emission	Cluster in nebula, dominated by gas emission	0	0	5	122	5	132
CN	Cluster with some emission	Cluster signature, dominated by stars	0	0	1	22	2	25
NA	Association in emission	Dominated by gas emission (mostly H II regions)	0	2	14	166	17	199
AN	Association with some emission	Dominated by stars	1	3	7	33	8	52
EN	Nebula without association or cluster	...	0	0	0	6	0	6
SNR	Supernova remnant	Type II SNRs trace star-forming regions	0	0	0	26	0	26
TDG	Tidal dwarf galaxy	Concentrations of objects in the Bridge	0	0	0	3	0	3
Total			961	214	119	1351	96	2741

The following objects from the Hodge & Wright (1974), Bruck (1975, hereafter B), and BS95 catalogs are not CAROs, and therefore are not included in Table 2: (i) HW7, HW17, and B141 are bright galaxies; (ii) H86-65, H86-66, B30, and B84 are galaxies with counterparts in the NASA/NED/IPAC extragalactic database; and (iii) BS 1 is a faint galaxy group. BS95 provided a list of faint entries of the B and H86 catalogs that were doubtful with the available means at that time. The present analysis using DSS and MAMA *J* images retrieved 12 B and 31 H86 clusters or candidates (Table 2).

We report some newly discovered faint clusters and candidates in the SMC (45 objects) and Bridge (19 objects). The objects were classified from their visual contrast in the MAMA *J* images, as illustrated for six of them in Figure 10 in Appendix A.

2.1. Cataloging Procedures

The present catalog follows the analysis of its recent Milky Way counterpart including 10978 CAROs (Bica et al. 2019, hereafter BP19). In order to reveal the nature of these objects, we consider their positions in equatorial coordinates, angular sizes, stellar densities, contrast to the field, contaminants, presence of cluster pairs or multiplets, hierarchical effects, shape, and astrophysical parameters, when available. Here hierarchy means that one object is included in another, e.g., a cluster inside an association, so the cluster is contained in the association.

These procedures were also applied to the BS95, Bica & Dutra (2000), and Paper I catalog versions. Compared with Paper I, the present data provide deeper material for the SMC main body and surroundings. In this work, we employed the DSS *B*, *R*, and *I* atlases, where *R* is the filter most sensitive to atomic line emission, and *I* is basically free of emission lines. The co-added multicolor DSS atlas and the *Spitzer* co-added bands are deeper. Particularly deep among the newly available surveys are the MAMA/SERC plates. In the outer parts of the SMC/MB, the recent cluster searches with the Optical Gravitational Lensing Experiment IV (OGLE-IV; Sitek et al. 2017) and Survey of the MAGellanic Stellar History (SMASH; Piatti 2017) are in general deeper than the DSS (available via the Aladin¹¹ software). In this case we cross-identified and incorporated them.

Table 2 includes 1447 entries corresponding to the updated literature, including the ones from the Bitsakis et al. (2018) catalog, which are treated in Section 3. Column 1 provides the designations in chronological order, so that discoveries can be verified. Rediscoveries are not a demerit, since they reinforce an object detection independently by different authors (BP19). Columns 2 and 3 give the J2000 right ascension (R.A.) and declination (decl.), respectively. Compared to Paper I, we now provide the time second decimal of the R.A. We measured this value for essentially all clusters and small associations. Earlier SMC and LMC catalogs were based on photographic plates obtained by different authors who derived approximate coordinates. The DSS plates with astrometry started to change that to a new paradigm (Bica et al. 2008a, and references therein). Nowadays, Aladin makes available digital surveys, either from plates, CCDs, or other detector surveys with good astrometric accuracy. However, crowding and saturation effects inhibit attempts to find centers automatically by stellar statistical techniques or flux peak fits, such that in some recent studies based on automatic searches, the coordinates may correspond to off-center positions. For detailed barycenter studies, higher resolution observations are needed, e.g., with the Adaptive Optics Module (SAM) on the Southern Astrophysical Research (SOAR) Telescope from the ground, or with the *Hubble Space Telescope* (*HST*). Visual inspection on survey images is a reliable method to systematically estimate cluster centers for catalogs, in particular in cases of crowded fields. In the present analysis, all the clusters have centered coordinates. Since for large associations and stellar/nebular complexes this time second decimal becomes irrelevant, we simply appended zero as decimal to such Paper I objects.

The object classes in column 4 (C, A, CA, AC, NA, AN, NC, CN, EN) and SNRs are the same as defined in Paper I, and are explained in Table 3. For more details on this classification, see Paper I. A new class is added: cluster candidate (CC). The catalog also contains three tidal dwarf galaxies (TDGs; Paper I). The number counts of these objects in the present catalog are also given in Table 3.

Major and minor angular sizes in columns 5 and 6 are guiding values measured by ourselves, estimated visually directly on the plates, or directly taken from other studies with deeper observations, which in general follow similar procedures to measure diameters. The objective is to provide basic information to compare the objects in view of selection criteria for future detailed studies. Column 7 refers to the present

¹¹ <https://aladin.u-strasbg.fr/>

classifications of the Bitsakis et al. (2018) objects as defined in Section 3. Columns 8 and 9 give the ages and metallicities compiled as described in Section 5, and columns 10 and 11 list the corresponding references. Comments in column 12 provide additional information such as hierarchical relations (e.g., in or include) or whether the object appears in a pair or multiplet, as for example a cluster present in an association.

During the verifications of new literature objects in DSS and MAMA J images, one of us (E. B.) checked Hodge’s faint clusters (Hodge 1986). During this verification, new similar clusters and cluster candidates were detected, using MAMA and the color BRI combined images in Aladin: 45 in the SMC, which we named SBica, and 19 in the Bridge area, analogously named BBica. These discoveries are incorporated in Table 2 and some of them are shown in Figure 10 in Appendix A.

Piatti & Bica (2012) analyzed frames from the Blanco 4 m telescope, obtained with a CCD camera equipped with Washington filters to study Hodge (1986) faint cluster candidates in the SMC central bar. Part of them were confirmed not to be clusters by means of color–magnitude diagrams (CMDs). We indicate them as “Ast” in the comment field (Table 2), indicating their probable nature as asterism. However, it would be important to observe them deeper because they may be counterparts of Galactic open clusters, not yet sampled in large numbers in the Clouds. We recall that Santiago et al. (1998) detected two faint counterparts of Milky Way open clusters using serendipitous *HST* observations of a rich field on the east side of the LMC bar.

3. Cross-identification with the Bitsakis et al. SMC Catalog

Bitsakis et al. (2018, hereafter **BGB+18**), provided the largest sample of SMC objects in the last decade (Table 1). We cross-identified their objects with the literature (Section 2). They employed a code that automatically detects overdensities above a local threshold. Monte Carlo simulations probed the background and the code detected both compact and diffuse overdensities. They calculated their ages by CMD fitting in the $(U - V)$ versus V , $(B - V)$ versus V , and $(V - i)$ versus i diagrams. However, for older clusters the data they use do not reach the turn-off, resulting in uncertain age determinations. They analyzed the following three databases: (i) SMC main body with the *Galaxy Evolution Explorer* (*GALEX*) in the near-UV ($\lambda_{\text{eff}} = 2175 \text{ \AA}$); (ii) central parts of the SMC in the *Swift*/Ultraviolet/Optical Telescope (*UVOT*) Magellanic Clouds Survey with the near-UV filters UV W1, W2, and W3; and (iii) the SMC main body with *Spitzer*/Infrared Array Camera (IRAC) $3.6 \mu\text{m}$. They designated the objects with the acronyms SMC-NUV, SMC-M2, and SMC-IR1, respectively. For the sake of simplicity and space, we abbreviated them in the present catalog to BUS, BMS, and BIS, respectively. The “B” in these acronyms refers to Bitsakis and “S” to the SMC, as usual in several catalogs (Table 1, Paper I).

BGB+18 referred to their detected objects as star clusters. The publication of such a cluster sample in excess of 1000 entries was surprising, and it would have an enormous impact on cluster luminosity functions. Piatti (2018) argued that the unprecedented number of new clusters could be greatly overestimated. In order to clarify this issue, we inspected the **BGB+18** objects taking into account the procedures in Section 2.1, and determining their angular separations to known objects from the literature and to each other. We searched for counterparts of the objects in **BGB+18** to test the

reliability of this selection and to collect additional information for the nature of these objects. The counterparts were verified using a number of criteria, including angular separation, diameters, classifications, and checking the DSS and MAMA J images. Most of them are located at less than $60''$ from known objects. Their decreasing number for separations larger than that ensures that we tested the bulk of near coincidences in the positions. The Bitsakis objects were here classified as follows.

- (i) 961 type “T” corresponding to isolated objects in column 7 of Table 2. As a rule they are extended, diffuse, and with low stellar densities, corresponding to properties of associations in the Clouds (e.g., Hodge 1985, BS95). In particular, they do not correspond to a typical faint cluster appearance (Hodge 1986). We conclude that such objects are to be classified as associations. In fact, many of them are not clearly seen on DSS or MAMA images, such that we cannot exclude the possibility that they are field fluctuations. This might be due to the fact that they used particular near-UV and IR material, having detected overdensities therein, but have no clear counterpart in the optical. Assuming these objects to be real, we decided to include all such **BGB+18** objects in the association class, which are readily discernible in our Table 2, column 4.
- (ii) 214 objects build pairs with other objects from our catalog, but are not similar enough to these to be considered the same object. We classify them as “N,” referring to nonsimilar,
- (iii) 119 objects have counterparts in the literature with comparable size and description. For this class we use the designation “E,” which stands for equivalent. Most of them are previously cataloged bright and moderately bright compact clusters. For the first time, the names of **BGB+18** objects with counterparts in the literature are explicitly given in the same catalog line, as suggested by Piatti (2018). Finally, we detected some equivalencies among objects from their three databases (BUS, BMS, and BIS), and to a lesser extent within the same database. These internal duplications are included in Table 2.
- (iv) 1351 objects in our catalog have no relation to any object in the **BGB+18** sample. We classify them as “U” (unrelated).
- (v) Yet, 96 objects are hierarchically related to the **BGB+18** objects, so we classified them as “R,” meaning related entries.

In conclusion, the diffuse **BGB+18** objects amount to 1175 (43% of the present overall catalog), corresponding mostly to associations. Their 119 compact objects are previously cataloged bright and moderately bright clusters. In essence, they have no faint clusters. Their determinations indicate a considerable fraction of ages over 100 Myr, thus older than typical OB associations. This suggests the occurrence of evolved associations and/or cluster dissolutions. Finally, the entries BIS767 and BUS486 were excluded because they are part of the Milky Way globular cluster NGC 362.

We point out that the objects in Table 2 span a wide range in size, class, and stellar or gas content. The previous literature cited from BS95 to the present paper show definitions and images of the different classes. We suggest the use of the present accurate coordinates and other characterizations for preliminary analyses to select object samples for observations.

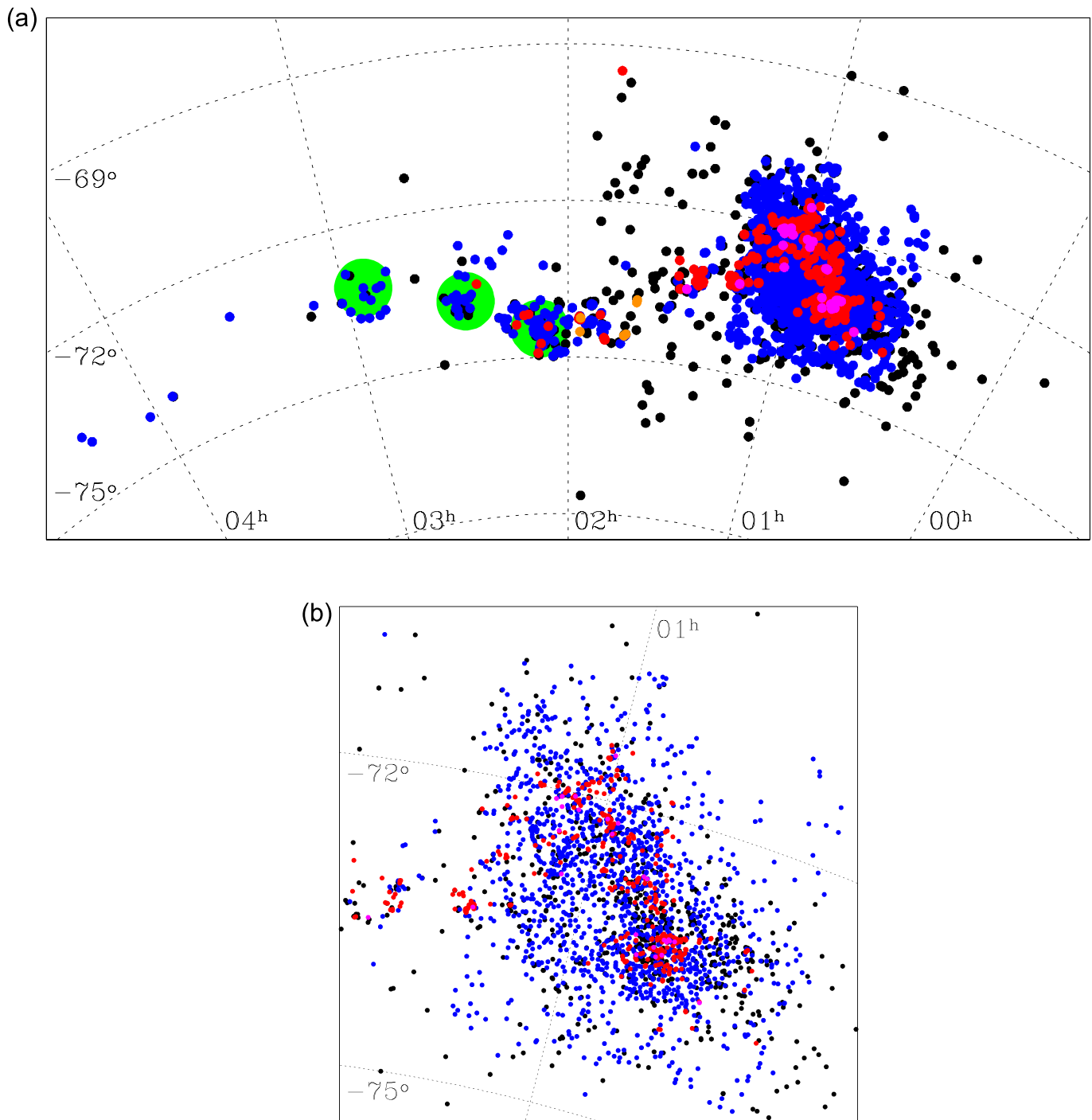


Figure 1. (a) Angular positions of the general catalog objects. Points are (i) black: star clusters (C, CA, CC), (ii) blue: associations without emission (A, AC), (iii) red: clusters and associations related to emission (NC, NA, AN, CN), (iv) magenta: SNRs, (v) orange: ENs, and (vi) finally, the three TDGs are the large green circles. (b) Enlargement of the most crowded region of Figure 1, the SMC main body, with smaller point sizes.

4. Properties of Objects in the Updated Catalog

We finally present a merged cross-identified new general catalog of CAROs in the SMC and MB, with 2741 entries. Figure 1 shows the angular positions of the six grouped object classes: clusters (C, CA, CC), emissionless associations (A, AC), clusters and associations with emission (CN, NC, AN, NA), SNRs, ENs, and TDGs (see Table 3 and Paper I for a description of these classes). ENs are emission nebulae without any obvious association or cluster. The star-forming regions in

the SMC main body, Wing, and Bridge are evident. Figure 1 illustrates a good definition of the SMC halo clusters owing to their increase in number. Both the star formation burst throughout the main body, Wing, and Bridge, and the inflated halo are part of the same phenomenon: the SMC disruption in the last (or last few) encounters with the LMC (e.g., Dias et al. 2016; Paper I; BP19). The new OGLE-IV and SMASH clusters in the SMC halo and Bridge are important to be studied in detail to disentangle Bridge young clusters from tidally stripped halo or disk clusters in the Clouds.

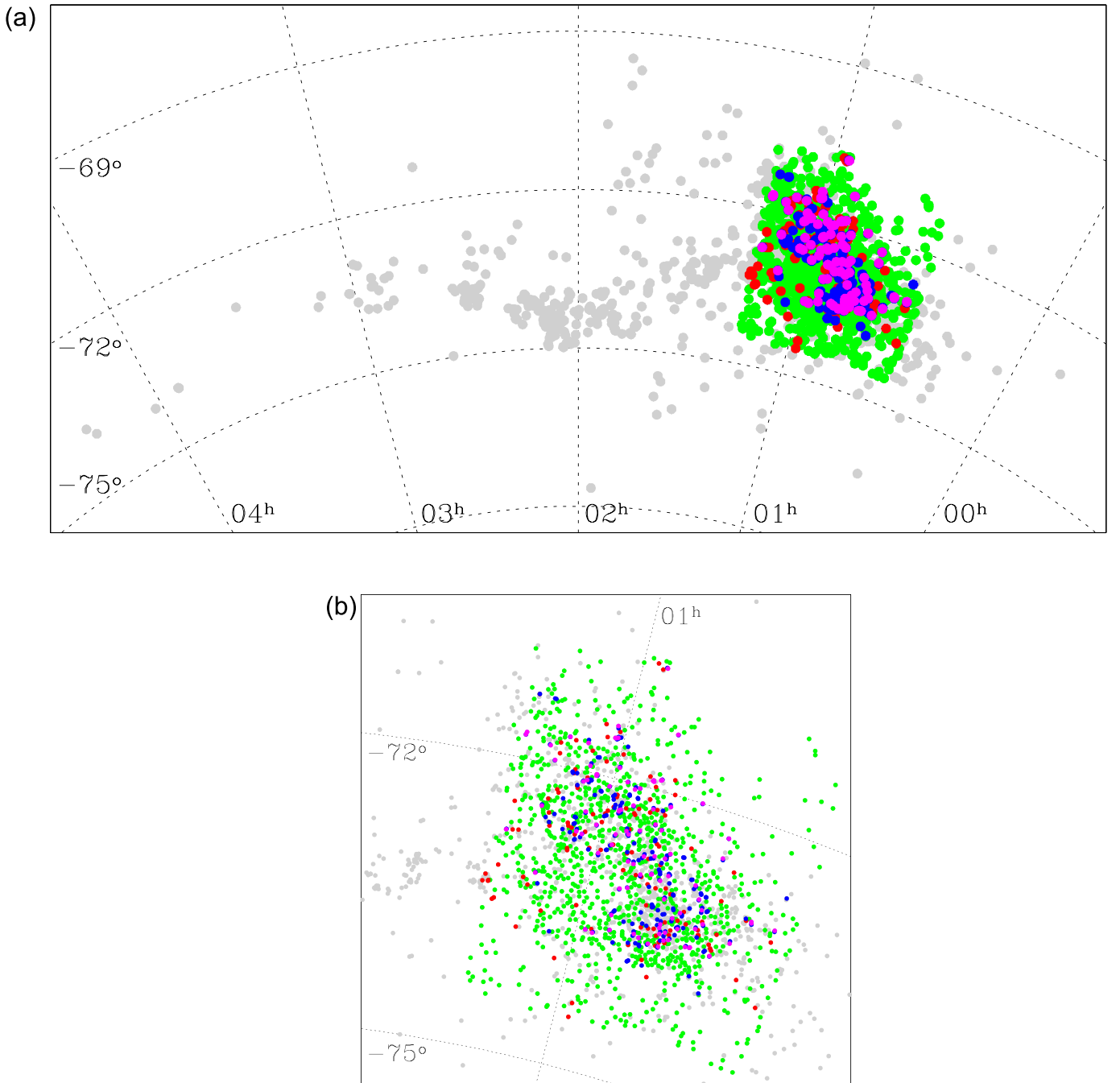


Figure 2. (a) Comparison with BGB+18: (i) gray points: present sample; (ii) green: 961 isolated objects (new associations); our BGB+18 catalog correlation class “I”; (iii) blue: their 214 objects, mostly associations, separated from literature entries by less than $60''$, class “N”; (iv) red: their 119 clusters with counterparts in the literature, class “E”; and (v) in magenta: 96 SMC objects in the literature not equivalent, but apparently related to the BGB+18 objects, class “R.” (b) Enlargement of the most crowded region of Figure 2, the SMC main body, with smaller point sizes.

Figure 2 shows the angular positions of the catalog objects, color coded by their relations to the BGB+18 sample, where the “I,” “N,” “E,” “U,” and “R” classes are as defined in the previous section.

Table 3 gives an updated census of the object classes and their counts, including different classes of correlation with the BGB+18 catalog. These classifications allow to peer and discriminate the new catalog contents, and have been used in several studies of the Clouds (Bica et al. 2008a, and references therein). The present general catalog is a factor ~ 2 larger than its Paper I counterpart.

5. Metallicities and Ages

Table 2 also includes in columns 8 to 11 a compilation of ages and metallicities from the literature, together with corresponding references and abbreviations. Since they include the results of BGB+18, it is the most complete sample available.

For the cases where more than one reliable age determination was available, we took the average in $\log(\text{Age})$. HW41, B112, and HW81 have double structures, so we do not include the single object ages. Since H86-106 may have two components, we do not include the age from the literature either.

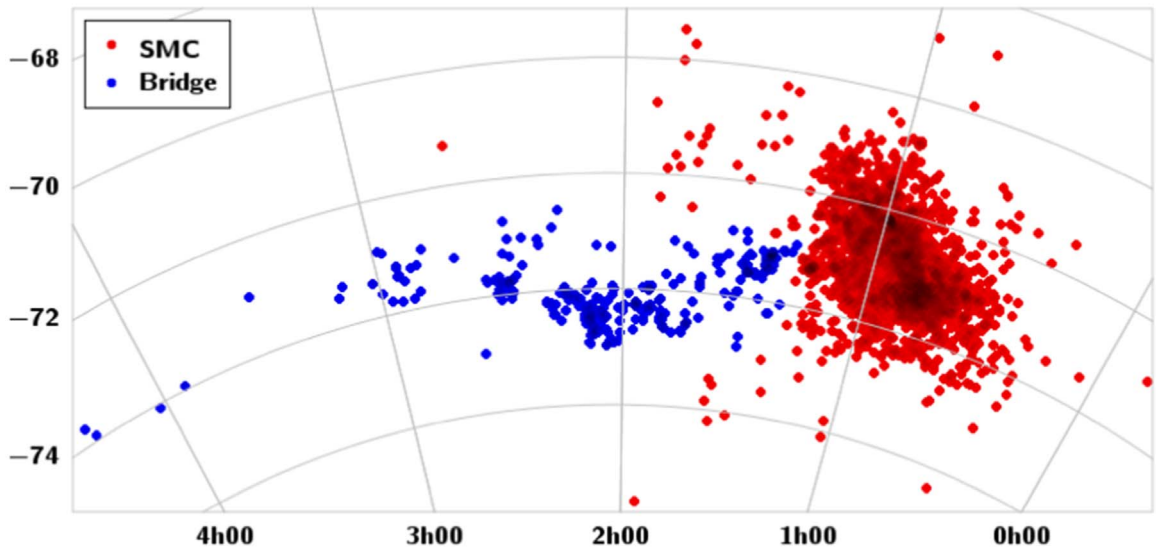


Figure 3. Separation of the SMC objects into main body (red) and Bridge + Wing (blue) samples.

For the metallicities, we selected the most reliable determinations, favoring, in this order: calcium triplet and other high-resolution spectroscopic determinations from individual (giant) stars, isochrone fitting in the CMD, in a few cases integrated spectroscopy, and if no other metallicity determinations were available, the Bica et al. (1986) integrated photometry values. For each object, the age and metallicity references are given in columns 10 and 11 of Table 2.

In Figure 3, the positions of the catalog objects with literature age and/or metallicity determinations can be seen, color coded by different ranges of these parameters. As an aid to see where they are located with respect to the LMC or Bridge, we show the objects without known age or metallicity in gray.

Figure 4 shows the CAROs identified as Bridge/Wing. For the sake of simplicity, we considered as belonging to the Bridge the objects between $1^{\text{h}}20^{\text{m}} < \text{R.A.} < 4^{\text{h}}30^{\text{m}}$ and $-75^{\circ} < \text{decl.} < -72^{\circ}$, thus including the SMC Wing.

Figure 5 shows the histogram of metallicities, separated as belonging to the SMC or Bridge+Wing. Among the 2741 entries, 626 are confirmed clusters, and metallicity derivations are mostly based on some of these clusters that amount to 117, plus a few associations. Therefore, only 134 clusters and associations (5%) have spectroscopic metallicities in the literature, whereas ages are available for 75% of them.

Testing statistical techniques to select the optimal bin width, we adopted the square root of the number of clusters, obtaining 11 bins of 0.2 dex. Of the 26 objects presented in the most metal-rich bin ($-0.2 < [\text{Fe}/\text{H}] < 0.0$, all from Perren et al. 2017), 12 objects have $[\text{Fe}/\text{H}] = -0.01$, which is the upper limit of the parameter space explored by them. If these objects were excluded from the analysis, this most metal-rich bin would then drop by half. The metallicity distribution presents a peak at $[\text{Fe}/\text{H}] \sim -0.8$ to -1.0 . This is in general terms in agreement with the recent literature on the stellar populations of the SMC: a mean metallicity of $[\text{Fe}/\text{H}] \sim -0.7$ is identified for the young populations (Karakas et al. 2018) and metallicities of $[\text{Fe}/\text{H}] \sim -0.8$ to -1.0 are assumed for red giant stars (D’Onghia & Fox 2016).

Parisi et al. (2015) found a metallicity distribution of clusters based on Ca II triplet spectroscopic metallicity ranging from $-1.4 < [\text{Fe}/\text{H}] < -0.4$ with a possible bimodality. Nevertheless, a non-negligible number of clusters are more metal-poor

than $[\text{Fe}/\text{H}] < -1.5$, and ~ 50 other ones are more metal-rich than $[\text{Fe}/\text{H}] > -0.5$. Recently a photometric metallicity map of the SMC was presented by Choudhury et al. (2018), showing no field stars with $[\text{Fe}/\text{H}] < -1.2$ and $[\text{Fe}/\text{H}] > -0.7$. Since this technique is limited to find more metal-poor stars, spectroscopy is required. Parisi et al. (2016) found a distribution of metallicities for field stars ranging from $-2.4 < [\text{Fe}/\text{H}] < -0.2$, based on Ca II triplet spectroscopy. Even considering that clusters could be captured from the LMC or from the Galaxy, and the low-metallicity and high-metallicity ones could be explained in that way, we would suggest that such clusters should be reanalyzed with high-resolution spectroscopy.

In Figure 6 the histogram of ages is shown, with a fixed bin width of 0.2 in $\log(\text{Age})$. It is interesting to note that a large number of them, amounting to 225 objects (of a total of 2019 objects or 75% of the sample), are older than 1 Gyr, which makes this sample of great interest for studies of the early formation of the SMC.

The age histogram suggests a major event of star formation at around 180 Myr, as could have been triggered by an encounter between the SMC and the LMC. This is the estimated age of the MB based on dynamical studies of the last encounter between LMC and SMC (e.g., Zivick et al. 2018). Looking at the histogram in blue where only Bridge objects are represented, it is clear that the star formation was quiescent until about ~ 150 Myr ago. However, the decay for $t > 500$ Myr clusters can be eroded by cluster dissolution effects, as in the Milky Way (Bonatto & Bica 2011). Old low-mass clusters are either too faint or have mostly been dissolved (Bonatto & Bica 2012).

The AMR of the SMC CAROs has been subject of considerable investigation. Parisi et al. (2015) have found that even with a homogeneous sample, there is an intrinsic metallicity dispersion at a given age, concluding that no single chemical evolution model can describe the evolution of the SMC. Dias et al. (2014, 2016) proposed to conduct this study by splitting the SMC into four groups related to the SMC-LMC-Milky Way tidal interactions, namely, the main body and three external groups that are being stripped out from the main body: Wing/Bridge, counter-bridge, and west halo. They pointed out the need of a homogeneous sample of ages and metallicities to make any reliable conclusions. Although we could not find a dip in metallicity in the AMR of the Wing/Bridge clusters in our sample, probably due to the highly

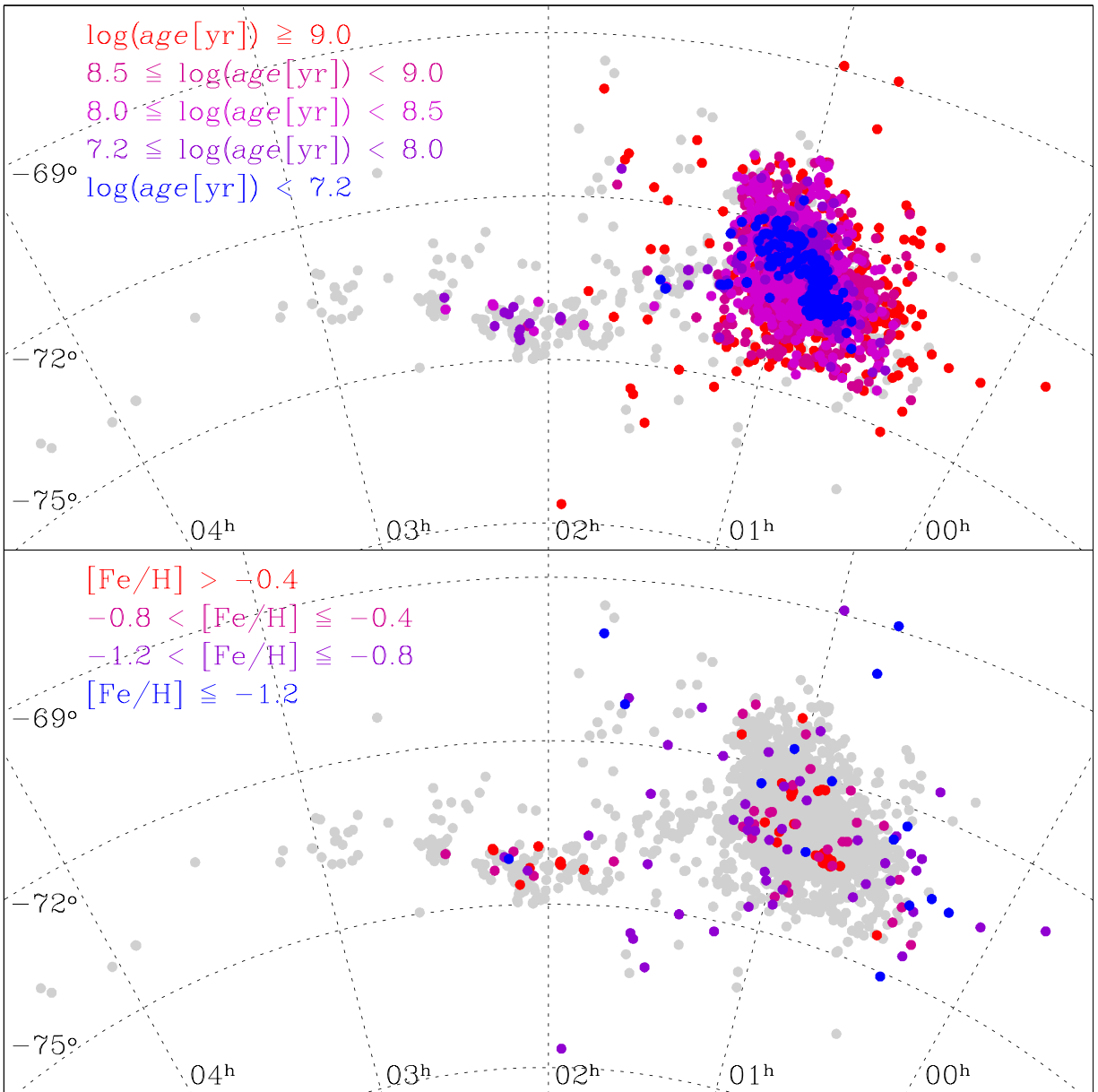


Figure 4. Spatial distribution of the ages and metallicities for the objects in the catalog. Objects in gray have no age or metallicity value in our catalog.

heterogeneous sample, as can be seen in Figure 7, we were still able to recover the inversion in the age and metallicity radial gradients found in the aforementioned works, as shown in Figure 8. We highlight the Wing/Bridge clusters and conclude that the inverted gradient out of $a \gtrsim 4^\circ$ seems to be dominated by Wing/Bridge clusters. A further detailed study with a homogeneous sample will be carried out in a future work.

6. Distant Clusters and New Outer Limits for the Magellanic System

Discoveries of ultra-faint star clusters (UFC) and ultra-faint (UFG) and faint (FG) dwarf galaxies around the Clouds have been mostly carried out with DES (Drlica-Wagner et al. 2015). Deep photometric, spectroscopic, kinematical, and dynamical follow-ups probed them further (e.g., Conn et al. 2018). The UFCs can be used to establish new landmarks and frontiers for an EMS. The catalog of the SMC/MB objects must cope with

that involving the Milky Way, LMC, and SMC potentials. The Milky Way has certainly captured clusters that originated in the LMC and SMC, and some of their satellite galaxies. The relevant FGs and UFGs are projected around the Clouds at various heliocentric distances, in front or behind them. They are or were LMC satellites (Jerjen et al. 2018, and references therein; Li et al. 2018). The UFCs Pic I and Phe II, as well as the UFG Grus I, present tidal substructures pointing to the LMC. The UFGs Hor I, Car II, Car III, and Grus I have been suggested to be related to the LMC, while Tuc II and Tuc IV might be related to the SMC, together with the UFCs DES 1 and Eri III (Conn et al. 2018). The UFG Hydrus I probably originated together with the LMC and migrated to the Milky Way halo (Koposov et al. 2018), while Grus I was probably captured by the Milky Way on the MC far side. Figure 9 shows the angular distribution of the objects in Table 4 (Appendix C) from the east in the LMC Leading Arm to far west of the SMC, trailing the MC. The present discussion deals with the entire

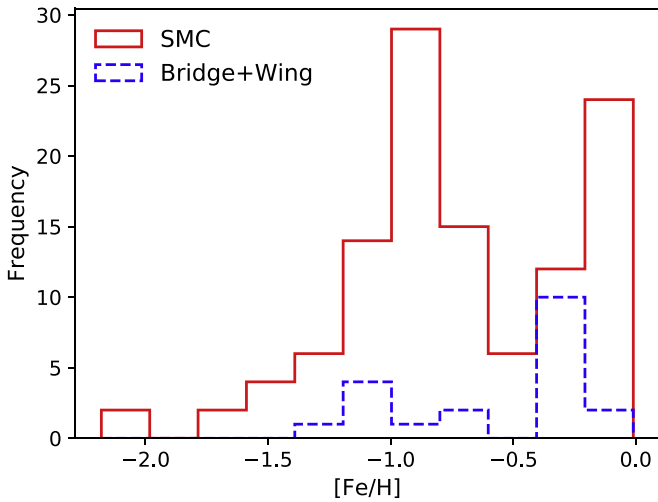


Figure 5. Histogram of metallicities in bins of 0.2 dex, subdivided in SMC and Bridge + Wing clusters.

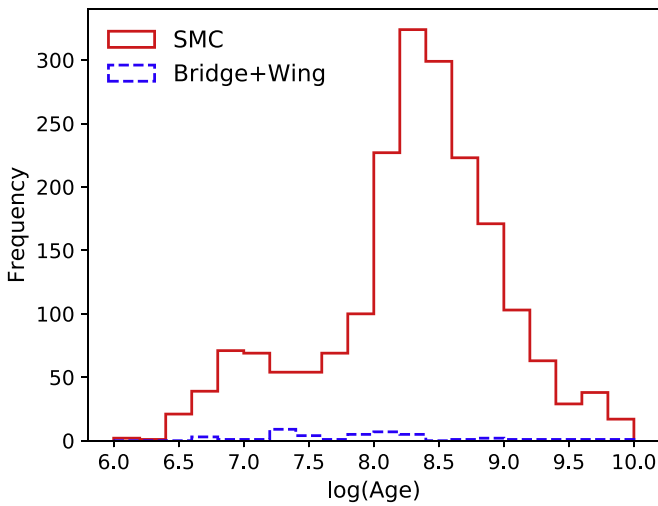


Figure 6. Histogram of ages, subdivided in SMC and Bridge + Wing clusters.

EMS, to be joined by the updated LMC catalog in a forthcoming study.

The LMC UFG neighbors, whether satellites, captures, dissolving, or comoving, can provide constraints on the formation and hierarchical evolution of galaxies (Dooley et al. 2017). Table 4 (Appendix C) gives 27 objects, their characterizations and references, containing UFCs, FGs, UFGs, tidal galaxies, and/or tidal debris. Several scenarios can operate: (i) co-movers with the Clouds in the Vast Polar Structure (VPO; Pawlowski & Kroupa 2014), (ii) satellites formed in or around the Clouds and eventually captured by the Milky Way, (iii) objects originated in the MC and captured by the Milky Way, and (iv) plain clusters that originated in the LMC or SMC that remain captive. In the last column of Table 4 we also show diagnostics on the object nature according to each paper, based on position, age, metallicity, total absolute magnitude, dark matter content, and/or orbits. In some cases we complemented them. The objects are contained in an area with an angular separation $<40^\circ$ from the LMC and heliocentric distances of $15 \text{ kpc} < d_\odot < 130 \text{ kpc}$. It includes a considerable Milky Way halo slice and engulfs the possibility of scattered objects with d_\odot a factor ~ 2 of the SMC and LMC distances of

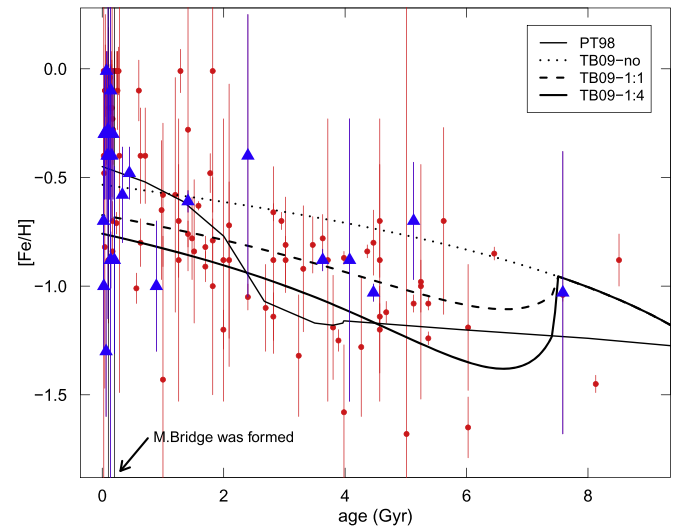


Figure 7. Age–metallicity distribution of SMC CAROs with information compiled in Table 2. The error bars represent the errors given by the respective authors. The Wing/Bridge clusters are shown as blue triangles. The formation time of the MB is indicated by vertical lines at 100–200 Myr (e.g., Zivick et al. 2018). The burst model of Pagel & Tautvaišienė (1958) and the merger models of Tsujimoto & Bekki (2009) are shown to illustrate how a single model is unable to reproduce the age–metallicity distribution of SMC CAROs.

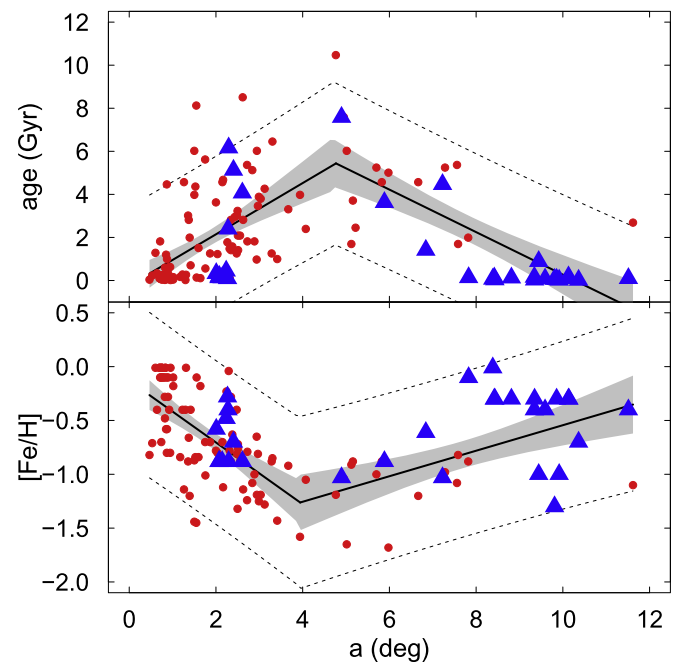


Figure 8. Age and metallicity of SMC clusters from the literature compilation in Table 2, as a function of the projected distance from the SMC center. The distance is the semimajor axis of the ellipse surrounding the SMC main body as defined by Piatti et al. (2007) and used by Dias et al. (2014, 2016) and Parisi et al. (2016). Bridge clusters are highlighted as blue triangles. The shaded gray area represents the 95% confidence interval of the fitted parameters. The dashed lines represent the 95% prediction interval of the points. We fitted all points with a linear regression with a breakpoint using the R package segmented (Muggeo 2003) to highlight the inversion in both gradients at about $a \sim 4^\circ\text{--}5^\circ$.

59 and 49 kpc, respectively, derived from Cepheids (Gieren et al. 2018).

Figure 9 shows the objects of Table 4 and suggests relationships within the EMS. The tidal dwarf galaxies BS I, BS II, and BS III (Paper I) in the Bridge may evolve to SMC Northern Over-Density (SMCNOD)-like (Pieres et al. 2017)

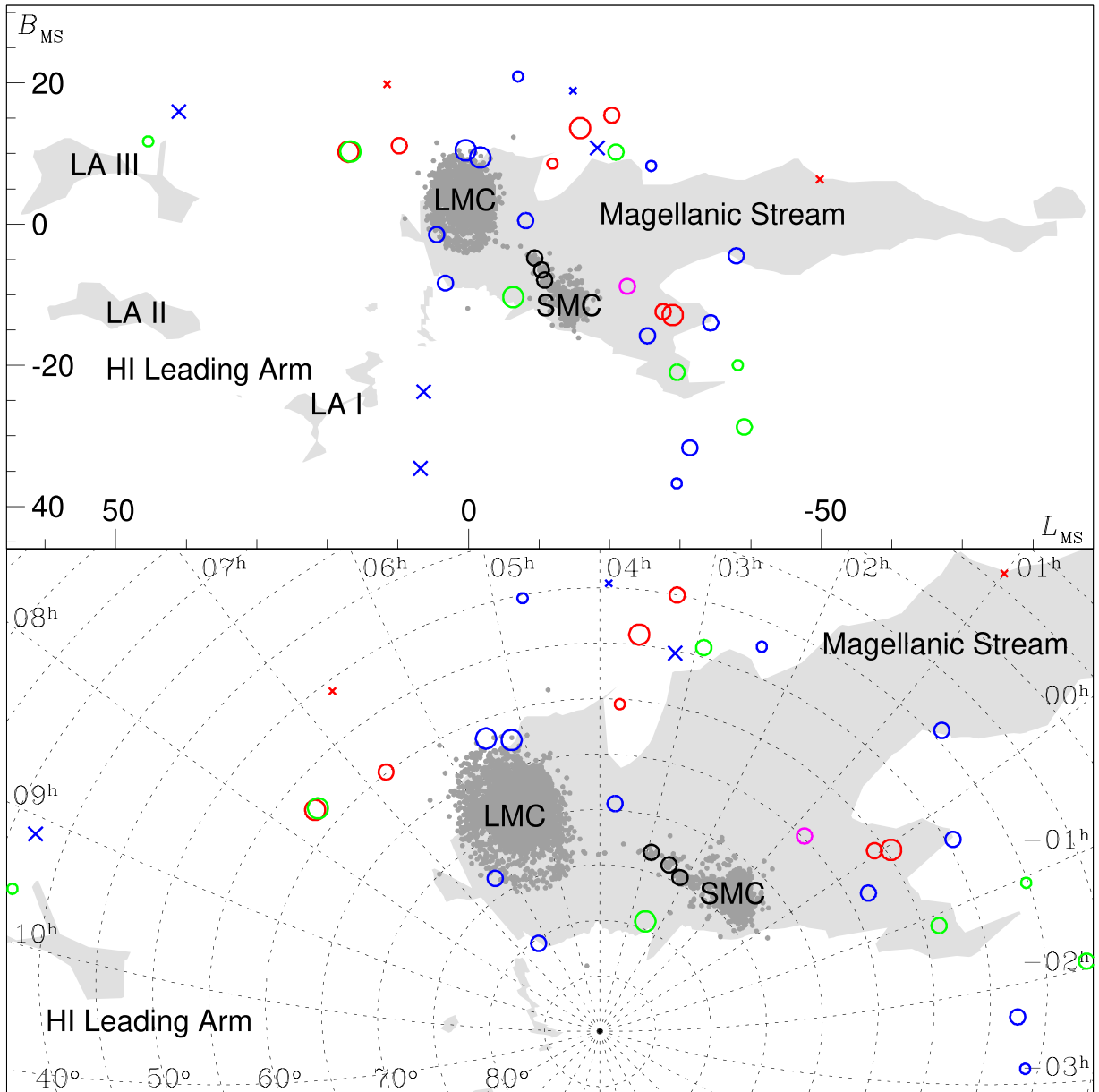


Figure 9. EMS angular distribution. Grey points: the present SMC/MB catalog and LMC CAROs from Paper I; blue: ultra-faint star clusters (UFCs); red: ultra-faint dwarf galaxies (UFGs); green: faint dwarf galaxies (FGs); magenta: tidal debris SMCNOD; open black circles: tidal dwarf galaxies from BS95; red crosses: dwarf spheroidals; blue crosses: Milky Way globular clusters; large symbols: objects up to 40 kpc from the Sun; intermediately sized symbols: objects between 40 and 90 kpc; small symbols: objects from 90 kpc distance on; and shaded regions in light gray: the Magellanic Stream and the H I Leading Arm. The contours of these gas structures were extracted by one of us (B. D.) from Figure 8 of Nidever et al. (2008) to represent the gas distribution regions without any information on gas density or velocity. LA I, LA II, and LA III are the Leading Arm complexes I, II, and III identified by Nidever et al. (2008). Top panel: the EMS object sample in relation to the two gas structures. Here, we use the Magellanic Stream Coordinate System as defined by Nidever et al. (2008). Bottom panel: enlargement of the region, where the EMS object sample lies.

overdensities, which are long-lived tidal debris. While the BS TDGs are gas-rich with an essentially young stellar content (BS15), SMCNOD has an intermediate age population. They may be different evolutionary stages of a process creating tidal dwarf galaxies (BS15 and references therein). SMCNOD on the SMC side, as well as Antlia II (Torrealba et al. 2019b), which is probably related to the LMC Leading Arm, may be evolved examples of TDGs, or alternatively, tidal debris. On the other hand, Ant II may represent one of the most diffuse genuine early galaxies (Torrealba et al. 2019b).

Objects related to the LMC or SMC are not restricted to the area studied here, which is expected to englobe an EMS.

Kallivayalil et al. (2018) found that Hydrus I, Car II, Car III, and Hor I, which are within this area, have kinematics consistent with the LMC. Furthermore, Hydra II (outside the area), and especially Dra II (far outside), may be kinematically related to the LMC and deserve more analysis in the future. Orbit calculations can indicate complex interaction scenarios, e.g., for Tuc III, an UFG with a stream and projected near the SMC. It appears to have endured a close encounter with the LMC at 75 Myr ago (Erkal et al. 2018), when it was cast into the Milky Way halo, and is in dissolution. Table 4 indicates the objects that have kinematical (radial velocity or proper motion) or dynamical (orbital) information. Many of the UFCs and

Table 4
Possible Extended Magellanic System Clusters and Satellite Dwarf Galaxies

Designation(s)	J2000 R.A. (hh:mm:ss.d)	J2000 Decl. (Deg:':")	Class	D (')	d (')	d_{\odot} (kpc)	M_V (mag)	kin.	References ^a	Comments
(1)	(2)	(3)	(4)	(5)	(6)	(7)	(8)	(9)	(10)	(11)
Kim 2, Indus 1, Indus I, DES J2108.8-5109	21:08:50.0	-51:09:49	UFC	2.8	2.8	100	1.3	n	(1)	Milky Way halo, MC origin?
DES 3	21:40:13.2	-52:32:30	UFC	2.0	2.0	76	-1.9	n	(4)	Milky Way halo
Grus II, DES J2204-4626	22:04:04.8	-46:26:24	FG	12.0	12.0	53	-3.9	y	(1), (12), (13)	UFC? MC satellite?
Tuc II, Tucana II, Tucana 2, DES J2251.2-5836	22:51:55.1	-58:34:08	FG	20.0	20.0	57	-3.8	y	(1), (10), (13)	Less prob. LMC sat., trailing LMC?
Gru I, Grus 1, Grus I	22:56:42.4	-50:09:48	FG	3.6	3.6	120	-3.4	y	(1), (8), (10)	Milky Way Halo, MC origin? Trailing LMC
Tuc V, Tucana V, DES J2337-6316	23:37:24.0	-63:16:12	UFC	2.0	2.0	55	-1.6	n	(1), (6), (13)	Related to the SMC, dissolving?
Phe II, Phe 2, Phoenix II, DES J2339.9-5424	23:39:58.3	-54:24:18	UFC	2.2	2.2	81	-2.74	y	(1), (8), (11), (13)	UFG? former LMC?, LMC sat.? VPO?
Tuc III, Tucana III, DES J2356-5935	23:56:25.8	-59:35:00	UFG	12.0	12.0	25	-3.4	y	(1), (7), (10)	MC Satellite?
Tuc IV, Tucana IV, DES J0002-6051	0:02:55.2	-60:51:00	UFG	18.0	18.0	48	-3.5	y	(1), (12), (13)	UFC? MC Satellite: LMC
DES 1, DES J0034-4902	0:33:59.8	-49:07:47	UFC	8.0	8.0	74	-1.42	n	(6)	Related to the SMC
SMCNOD	0:47:59.9	-64:48:02	debris	360	180	62	-7.7	n	(9)	TDG? Disrupted SMC satellite
Eri III, Eri 3, Eridanus III, DES J0222.7-5217	2:22:45.5	-52:17:05	UFC	2.5	2.5	91	-2.07	y	(6), (13)	MC sat., LMC?
Hydrus I, Hydrus 1	2:29:33.4	-79:18:32	FG	13.0	13.0	28	-4.7	y	(1), (10)	Milky Way halo, LMC satellite. MC origin?
Hor I, Hor 1, Horologium I, DES J0255.4-5406	2:55:31.7	-54:07:08	FG	2.6	2.6	68	-3.58	y	(1), (8), (10), (13)	LMC satellite
Torrealba 1, To 1	3:44:19.8	-69:25:21	UFC	0.6	0.6	44	-1.6	n	(4)	LMC halo? Bridge? Stripped?
Hor II, Horologium II	3:16:32.1	-50:01:05	UFG	19.0	19.0	78	-2.1	y	(1), (5), (11), (13)	Pair with Hor I? LMC satellite
Ret II, Reticulum II, Ret 2, DES J0335.6-5403	3:35:47.8	-54:02:48	UFG	7.5	7.5	30	-2.7	y	(1), (10), (12), (13)	Less probable LMC satellite
Ret III, Reticulum III, DES J0345-6026	3:45:26.4	-60:27:00	UFG	4.8	4.8	92	-3.4	y	(1), (11), (13)	UFC? LMC Satellite
Pic I, Pictor I, Pictor 1, DES J0443.8-5017	4:43:47.4	-50:16:59	UFC	1.8	1.8	110	-2.05	y	(1), (8), (13)	LMC satellite
OGLL 863 ^b , DES 4	5:28:22.8	-61:43:26	UFC	1.7	1.7	31	-1.1	n	(14), (4)	In the LMC, GC? OC? UFG?
OGLL 874 ^b , DES 5	5:10:01.1	-62:34:49	UFC	0.4	0.4	25	0.3	n	(14), (4)	In the LMC
OGLL 845 ^b , Gaia 3	6:20:14.2	-73:24:52	UFC	1.1	1.1	48	-3.3	n	(14), (4)	In LMC: 1.3 Gyr, [Fe/H] = -1.8
SMASH 1	6:20:59.9	-80:23:45	UFC	5.5	5.5	57	-1.0	n	(3)	LMC cluster. LMC halo?
Pic II, Pictor II, MagLiteS J0644-5953	6:44:43.2	-59:53:49	UFG	7.6	7.6	45	-3.2	n	(1)	LMC Satellite, LMC origin
Car II, Carina II	7:36:25.6	-57:59:57	FG	17.0	17.0	36	-4.5	y	(1), (10)	LMC satellite
Car III, Carina III	7:38:31.2	-57:53:59	UFG	7.5	7.5	28	-3.4	y	(1), (10)	LMC satellite
Ant II, Ant 2, Antlia II, Antlia 2	9:35:32.8	-36:46:03	FG	150	150	130	-8.5	y	(2)	Milky Way sat., LMC Leading Arm? Debris?

Notes. The columns give, respectively, one or more designations; R.A. and decl. in J2000 epoch; major (D) and minor (d) axes in arcmin; distance to the Sun (d_{\odot}) in kiloparsecs; absolute magnitude M_V ; whether the object has studies about its kinematics or orbits (yes or no); and a references list and comments.

^a The numbers in the references list correspond to: (1) Kallivayalil et al. (2018); (2) Torrealba et al. (2019b); (3) Martin et al. (2016); (4) Torrealba et al. (2019a); (5) Kim & Jerjen (2015); (6) Conn et al. (2018); (7) Erkal et al. (2018); (8) Jerjen et al. (2018); (9) Pieres et al. (2017); (10) Fritz et al. (2018); (11) Fritz et al. (2019); (12) Massari & Helmi (2018); (13) Pace & Li (2019); and (14) Sitek et al. (2016).

^b OGLL are OGLE LMC objects from Sitek et al. (2016).

UFCs have kinematical/dynamical data, and in general they support a physical connection with the Clouds.

The Λ Cold Dark Matter theories predict that the halos of galaxies like the LMC should include about 50 dwarf companions (Dooley et al. 2017). Several of them appear to have been detected (Table 4). Despite the massive search efforts, there is a deficit of companion galaxies, while initially classified as UFG candidates turned out to be UFCs, as shown by follow-up studies, such as Eri III (Jerjen et al. 2018), Pic I, and probably Phe II (Conn et al. 2018). Table 4 contains 13 UFCs, 7 FGs, and 7 UFGs, when placing the limit between FG and UFG/UFCs at $M_V = -3.5$. LMC satellites are still missing (Dooley et al. 2017, present study). Possibilities are: (i) dwarf galaxy dissolutions have been frequent, as the MC plunged into the Milky Way halo; (ii) fainter galaxies will be discovered, especially UFGs or extended low density FGs like Ant II; (iii) or alternatively, some changes are needed in early universe models (Dooley et al. 2017).

Two dwarf spheroidals and five Milky Way halo globular clusters are located within the area studied here. Orbit calculations (Gaia Collaboration et al. 2018) showed that Sculptor resides between an apocenter of 111.8 kpc and a pericenter of 59.7 kpc, and Carina between 107.5 and 87.0 kpc. The pericenter suggests that Sculptor may have had interactions with the MC. Orbits of the five Milky Way halo globular clusters (Baumgardt et al. 2019) show that the apocenters of IC 4499 and NGC 1261 are smaller than 28 kpc, suggesting early accretions in the hierarchical history of the Galaxy. NGC 6101 with an apocenter at 47 kpc may have interacted with the LMC. NGC 6101, Pyxis [131.2, 26.3 kpc], and AM 1 [308.3, 98.8 kpc] require mass models including the MC for reliable interpretations.

Sitek et al. (2016) discovered clusters in the outskirts of the LMC, and Torrealba et al. (2019a) derived parameters for them. Thus we also include their OGLL designations in Table 4. They are projected near the edge of the LMC outer disk (Figure 9). *Gaia* 3 has a compatible distance to the LMC (Table 4), while DES 4 and DES 5 are located somewhat in the LMC foreground, suggesting capture by the Milky Way potential.

The 13 UFCs as an ensemble (Table 4, Figure 9) suggest that the EMS is very extended, and that most of them were formed in the Clouds and some others have migrated into the Milky Way potential well. However, the AMRs of the Clouds (Piatti & Geisler 2013) are not matched by the young age and low metallicity of OGLL 845 (*Gaia* 3), which appears to have its origin in another dwarf galaxy. Pic I is an UFC whose orbit indicates it as an outer LMC member. The Milky Way and especially the LMC still require more realistic model potentials (Erkal et al. 2018). Hammer et al. (2018) recently argued that the Galactic gravitational potential induces the dwarf line-of-sight velocity dispersion, questioning the estimates of dark matter. Table 4 gives hints, but to settle the EMS benchmarks, more constraints are necessary, both observational and theoretical.

7. Concluding Remarks and Perspective on Future Work

We provide an updated census of star clusters, associations, and other related extended objects in the SMC and MB. Ten years have elapsed since the last general catalog effort, and new cross-matches were necessary. Interesting new clusters have

been discovered in recent surveys, such as OGLE-IV (Sitek et al. 2017) and SMASH (Piatti 2017) in the SMC halo and Bridge, as well as VMC central SMC bar clusters in the near-IR (Piatti et al. 2016). We communicate our own discovery of 64 clusters and candidates in the SMC and Bridge.

We also cross-identified these clusters and candidates with objects from the SMC catalog by BGB+18. We clarified the issue of the overestimated number of star clusters (see Piatti 2018). BGB+18 refer to their objects as star clusters, but most have low stellar density and are in general diffuse and extended. Consequently, we classified them as associations. The census indicates that BGB+18 contributed with 1175 new SMC objects, while 119 have previous counterparts. Their sample contains essentially no faint clusters. All in all, the present general catalog provides 2741 objects in the SMC and Bridge (Table 2).

The present effort producing accurate coordinates and cross-matches for the previous literature objects will be useful for new cluster searches. An example is by means of image inspections by researchers and interested citizens, as organized by SMASH.¹² We point out that the present new clusters and candidates were not systematically searched for, but were mostly found serendipitously while analyzing the SMC and Bridge fields for previous objects. The new updated, reliable coordinates and characterizations will be particularly useful for observations, by minimizing uncertainties in crowded cluster zones, or in the study of cluster pairs and multiplets. It must be emphasized that the cluster center pointings in this paper provide in general more accurate cluster coordinates than previous studies because the latter searched for peaks in stellar or flux density distributions, which as a rule have shifts owing to overcrowding and saturation effects. The present catalog also contains ages and metallicities from the literature, where available.

As a continuation of this work we will present a study of the LMC, also starting off from Paper I and adding new studies by means of cross-identifications, in particular the LMC analysis of Bitsakis et al. (2017).

A general SMC catalog must address the numerous UFCs, FGs, and UFGs surrounding the Clouds. Table 4 compiles 27 such underluminous objects, providing diagnostics for their nature, and the probable relation to the Clouds or Milky Way. Most of the FGs and UFGs are compatible with being satellites of the Clouds, while UFCs appear to have originated in the Clouds.

The present study was carried out within the framework of the ongoing project VISCACHA (Maia et al. 2019). This project employs the SOAR 4.1 m telescope with instrumental settings determining the ages of massive and low-mass MC clusters from their CMDs, going deeper than the turn-off of old clusters in both Clouds, dealing better with crowding than previous surveys, because of the adaptive optics module SAM. Currently, we are facing the curtain of low-mass clusters in the SMC (e.g., Piatti & Bica 2012). However, we have not yet unveiled them to show clusters with masses comparable to open clusters in the Milky Way, as the two clusters serendipitously found with *HST* in a bar crowded field on the east side of the LMC (Santiago et al. 1998). The present effort to gather all known clusters so far into a single SMC and Bridge catalog with improved positions and other

¹² <https://www.zooniverse.org/projects/lcjohnso/local-group-cluster-search>

characteristics will be particularly useful to probe the hidden population of faint clusters in the Clouds. In return, the VISCACHA results, i.e., the properties of the observed stellar clusters, will be implemented into the catalog.

The authors acknowledge support from the Brazilian Institutions CNPq, FAPESP, and FAPEMIG. F.F.S.M. acknowledges FAPESP funding through the fellowship No. 2018/05535-3. R.A.P.O. acknowledges the FAPESP PhD fellowship no. 2018/22181-0. This study was financed in part by the Coordenação de Aperfeiçoamento de Pessoal de Nível Superior—Brazil (CAPES)—Finance Code 001.

This research has made use of the Aladin sky atlas developed at CDS, Strasbourg Observatory, France (Bonnarel et al. 2000;

Boch & Fernique 2014). We thank the anonymous referee for interesting remarks.

Appendix A New Clusters

In Figure 10 we show examples of newly identified clusters and candidates in the SMC main body and the Bridge. The mosaic shows $2' \times 2'$ images with MAMA J (Blue). From top left in the clockwise direction: SBica 12 is compact and barely resolved, SBica 25 is more resolved, and SBica 35 is compact. BBica 7 is a small cluster or a cluster core. BBica 1 suggests dissolution, and SBica 40 is small and loose.

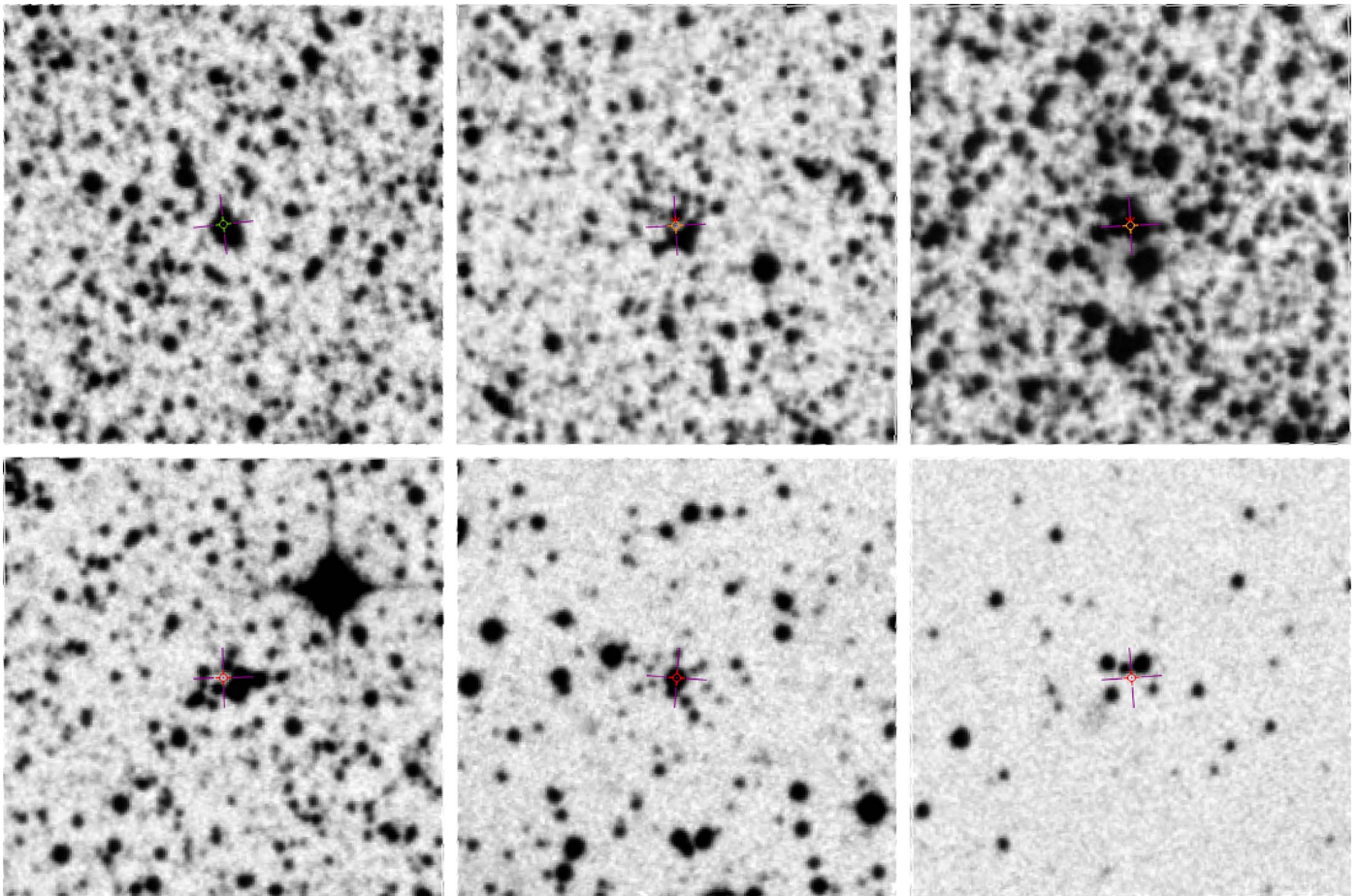


Figure 10. Mosaic showing newly identified clusters and candidates, obtained with the Aladin software, in panels of $2' \times 2'$. North is up, east is left. From top left in the clockwise direction: SBica 12, SBica 25, SBica 35, BBica 7, BBica 1, and SBica 40.

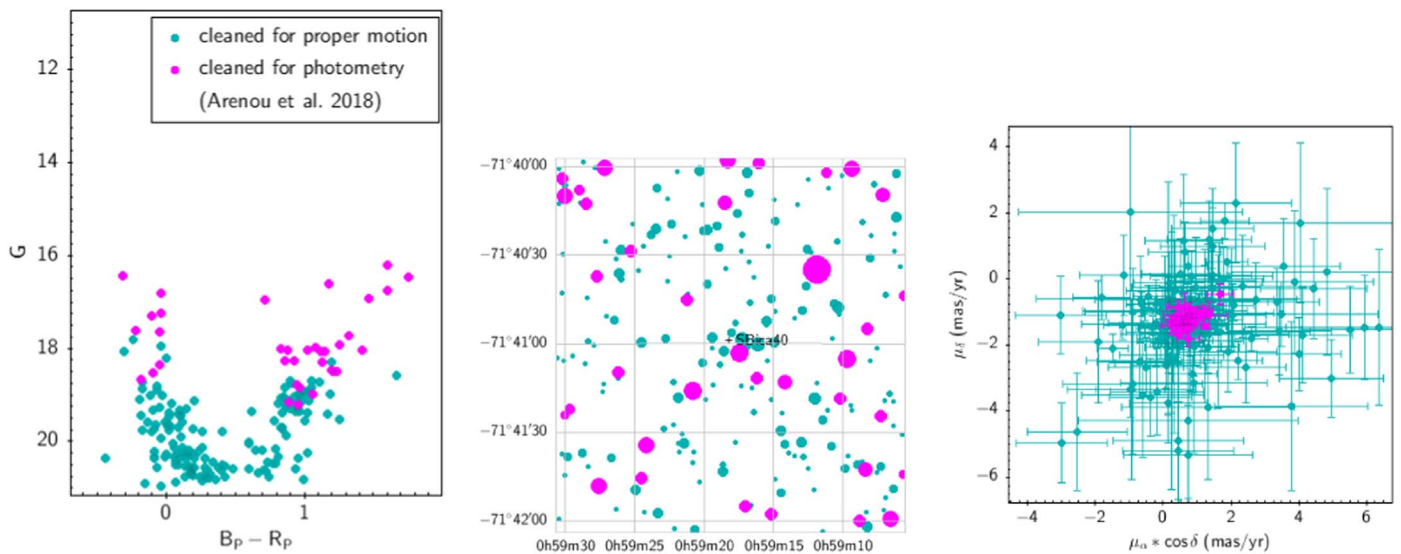


Figure 11. CMD (left), sky chart (middle), and VPD (right) of a $2' \times 2'$ sample around candidate cluster SBica 40, extracted from the *Gaia* catalog using quality constraints for photometry (magenta) or proper motion (cyan) usage (Arenou et al. 2018).

Appendix B Gaia Data

Photometry and astrometry from the *Gaia* second data release (DR2) were employed in an attempt to characterize some of the newfound cluster candidates. For this purpose, we have used Vizier¹³ to extract data inside a $2' \times 2'$ area centered on prominent SBica 40, matching the angular dimensions of Figure 10.

In order to properly filter bad-quality data for photometry purposes, we have followed the recommendations in Arenou et al. (2018), using their Equations (1) and (2) in order to remove poor astrometric solutions, spurious sources, and calibration problems. These filters have been consistently applied by many authors to produce reliable photometric analysis. On the other hand, when only a proper motion analysis is needed, Equations (1) and (3) are recommended instead, as these filters will retain a much larger fraction of the catalog and still be useful for astrometric purposes.

Figure 11 presents the analysis of the *Gaia* DR2 data for the SBica 40 area. It shows the resulting cleaned samples of *Gaia* data extracted around cluster candidate SBica 40, aiming at characterizing its stellar population. Although the proper motion sample has a significant number of stars, it can be seen that its uncertainties on the vector-point diagram (VPD) are too large to discriminate individual cluster movement from that of the general LMC and Galactic fields. Additionally, the distribution of the sample cleaned for photometry in both the CMD and on the sky chart is not sufficient to carry out a proper analysis of the target.

This analysis was also carried out in more populous clusters of the SMC, yielding similar results. Therefore, we concluded that the *Gaia* data is not suitable for carrying out a preliminary analysis of such faint clusters.

Appendix C

Possible EMS Clusters and Satellite Dwarf Galaxies

Table 4 lists the faint and ultra-faint clusters and galaxies (UFC, UFG, FG) populating the EMS. These neighbors include

satellites, captures, and dissolving and comoving objects in the vicinity of the Clouds. Their main characteristics (e.g., position, type, size, distance, brightness) and references are provided.

ORCID iDs

Pieter Westera <https://orcid.org/0000-0003-3379-994X>

Leandro de O. Kerber <https://orcid.org/0000-0002-7435-8748>

Bruno Dias <https://orcid.org/0000-0003-4254-7111>

Francisco Maia <https://orcid.org/0000-0002-2569-4032>

João F. C. Santos Jr. <https://orcid.org/0000-0003-1794-6356>

Raphael A. P. Oliveira <https://orcid.org/0000-0002-4778-9243>

References

- Alcaino, G., Liller, W., & Alvarado, F. 1996, *AJ*, **112**, 2004
 Alves, D. R., & Sarajedini, A. 1999, *ApJ*, **511**, 225
 Arenou, F., Luri, X., Babusiaux, C., et al. 2018, *A&A*, **616**, A17
 Badenes, C., Maoz, D., & Draine, B. T. 2010, *MNRAS*, **407**, 1301
 Baumgardt, H., Hilker, M., Sollima, A., & Bellini, A. 2019, *MNRAS*, **482**, 5138
 Bekki, K. 2012, *MNRAS*, **422**, 1957
 Belokurov, V., Erkal, D., Deason, A. J., et al. 2017, *MNRAS*, **466**, 4711
 Bica, E., Bonatto, C., Dutra, C. M., & Santos, J. F. C., Jr. 2008a, *MNRAS*, **389**, 678
 Bica, E., Dottori, H., & Pastoriza, M. 1986, *A&A*, **156**, 261
 Bica, E., & Dutra, C. M. 2000, *AJ*, **119**, 1214
 Bica, E., Pavani, D., Bonatto, C., & Lima, E. 2019, *AJ*, **157**, 12
 Bica, E., Santiago, B., Bonatto, C., et al. 2015, *MNRAS*, **453**, 3190
 Bica, E., Santos, J. F. C., Jr., & Schmidt, A. A. 2008b, *MNRAS*, **391**, 915
 Bica, E., & Schmitt, H. R. 1995, *ApJS*, **101**, 41
 Bitsakis, T., Bonfini, P., González-Lópezlira, R. A., et al. 2017, *ApJ*, **845**, 56
 Bitsakis, T., González-Lópezlira, R. A., Bonfini, P., et al. 2018, *ApJ*, **853**, 104
 Boch, T., & Fernique, P. 2014, in ASP Conf. Ser. 485, *Astronomical Data Analysis Software and Systems XXIII*, ed. N. Manset & P. Forshay (San Francisco, CA: ASP), 277
 Bonatto, C., & Bica, E. 2011, *MNRAS*, **415**, 2827
 Bonatto, C., & Bica, E. 2012, *MNRAS*, **423**, 1390
 Bonnarel, F., Fernique, P., Bienaymé, O., et al. 2000, *A&AS*, **143**, 33
 Bruck, M. T. 1975, *MNRAS*, **173**, 327
 Carlson, L. R., Sabbi, E., Sirianni, M., et al. 2007, *ApJL*, **665**, 109
 Carrera, R., Conn, B. C., Noël, N. E. D., et al. 2017, *MNRAS*, **471**, 4571

¹³ <http://vizier.u-strasbg.fr/>

- Chiosi, E., Vallenari, A., Held, E. V., Rizzi, L., & Moretti, A. 2006, *A&A*, **452**, 179
- Choudhury, S., Subramanian, S., Cole, A. A., & Sohn, Y.-J. 2018, *MNRAS*, **475**, 4279
- Cignoni, M., Cole, A. A., Tosi, M., et al. 2013, *ApJ*, **775**, 83
- Cignoni, M., Sabbi, E., Nota, A., et al. 2009, *AJ*, **137**, 3668
- Conn, B. C., Jerjen, H., Kim, D., et al. 2018, *ApJ*, **852**, 68
- Crowl, H. H., Sarajedini, A., Piatti, A. E., et al. 2001, *AJ*, **122**, 220
- da Costa, G. S. 1999, in *IAU Symp. 190, New Views of the Magellanic Clouds*, ed. Y.-H. Chu et al. (Cambridge: Cambridge Univ. Press), 446
- da Costa, G. S., & Hatzidimitriou, D. 1998, *AJ*, **115**, 1934
- D'Onghia, E., & Fox, A. J. 2016, *ARA&A*, **54**, 363
- de Freitas Pacheco, J. A., Barbuy, B., & Idiart, T. 1998, *A&A*, **332**, 19
- Demers, S., & Battinelli, P. 1998, *AJ*, **115**, 154
- Demers, S., Grondin, L., Irwin, M. J., & Kunkel, W. E. 1991, *AJ*, **101**, 911
- Dias, B., Coelho, P., Barbuy, B., Kerber, L. O., & Idiart, T. 2010, *A&A*, **520**, 85
- Dias, B., Kerber, L. O., Barbuy, B., et al. 2014, *A&A*, **561**, 106
- Dias, B., Kerber, L. O., Barbuy, B., Bica, E., & Ortolani, S. 2016, *A&A*, **591**, 11
- Dolphin, A. E., Walker, A. R., & Hodge, P. W. 2001, *ApJ*, **562**, 303
- Dooley, G. A., Peter, A. H. G., Carlin, J. L., et al. 2017, *MNRAS*, **472**, 1060
- Drlica-Wagner, A., Bechtol, K., Rykoff, E. S., et al. 2015, *ApJ*, **813**, 109
- Erkal, D., Li, T. S., Koposov, S. E., et al. 2018, *MNRAS*, **481**, 3148
- Fritz, T. K., Battaglia, G., Pawlowski, M. S., et al. 2018, *A&A*, **619**, 103
- Fritz, T. K., Carrera, R., Battaglia, G., & Taibi, S. 2019, *A&A*, **623**, 129
- Gaia Collaboration, Helmi, A., van Leeuwen, F., et al. 2018, *A&A*, **616A**, 12
- Gieren, W., Storm, J., Konorski, P., et al. 2018, *A&A*, **620**, 99
- Girardi, L., Chiosi, C., Bertelli, G., & Bressan, A. 1995, *A&A*, **298**, 87
- Glatt, K., Gallagher, J. S., III, Grebel, E. K., et al. 2008, *AJ*, **135**, 1106
- Glatt, K., Grebel, E. K., & Koch, A. 2010, *A&A*, **517A**, 50
- Glatt, K., Grebel, E. K., Sabbi, E., et al. 2008, *AJ*, **136**, 1703
- González Delgado, R. M., & Cid Fernandes, R. 2010, *MNRAS*, **403**, 797
- Gouliermis, D. A., Quanz, S. P., & Henning, T. 2007, *ApJ*, **665**, 306
- Grondin, L., Demers, S., & Kunkel, W. E. 1992, *AJ*, **103**, 1234
- Grondin, L., Demers, S., Kunkel, W. E., & Irwin, M. J. 1990, *AJ*, **100**, 663
- Hammer, F., Yang, Y., & Arenou, F. 2018, *ApJ*, **860**, 76
- Hill, V. 1999, *A&A*, **345**, 430
- Hodge, P. 1985, *PASP*, **97**, 530
- Hodge, P. 1986, *PASP*, **98**, 1113
- Hodge, P. W., & Wright, F. W. 1974, *AJ*, **79**, 858
- Jerjen, H., Conn, B., Kim, D., & Schirmer, M. 2018, *MNRAS*, submitted (arXiv:1809.02259)
- Kallivayalil, N., Sales, L. V., Zivick, P., et al. 2018, *ApJ*, **867**, 19
- Karakas, A. I., Lugaro, M., Carlos, M., et al. 2018, *MNRAS*, **477**, 421
- Kim, D., & Jerjen, H. 2015, *ApJL*, **808**, 39
- Koposov, S. E., Walker, M. G., Belokurov, V., et al. 2018, *MNRAS*, **479**, 534
- Kron, G. E. 1956, *PASP*, **68**, 125
- Kunkel, W. E. 1980, in *IAU Symp. 85, Star Cluster*, ed. J. E. Hesser (Dordrecht: D. Reidel), 353
- Li, T. S., Simon, J. D., Pace, A. B., et al. 2018, *ApJ*, **857**, 145
- Lindsay, E. M. 1958, *MNRAS*, **118**, 172
- Maia, F. F. S., Dias, B., Santos, J. F. C., Jr., et al. 2019, *MNRAS*, **484**, 5702
- Maia, F. F. S., Piatti, A. E., Santos, J. F. C., Jr., et al. 2014, *MNRAS*, **437**, 2005
- Martin, N. F., Jungbluth, V., Nidever, D. L., et al. 2016, *ApJL*, **830**, 10
- Massari, D., & Helmi, A. 2018, *A&A*, **620**, 155
- Mighell, K. J., Sarajedini, A., & French, R. S. 1998, *AJ*, **116**, 2395
- Mould, J. R., Jensen, J. B., & da Costa, G. S. 1992, *ApJS*, **82**, 489
- Muggeo, V. M. R. 2003, *Stat. Med.*, **22**, 3055
- Nidever, D. L., Majewski, S. R., & Butler Burton, W. 2008, *ApJ*, **679**, 432
- Pace, A. B., & Li, T. S. 2019, *ApJ*, **875**, 77
- Pagel, B. E. J., & Tautvaišienė, G. 1958, *MNRAS*, **299**, 535
- Palma, T., Clariá, J. J., Geisler, D., & Ahumada, A. V. 2015, *BAAA*, **57**, 102
- Parisi, M. C., Geisler, D., Carraro, G., et al. 2014, *AJ*, **147**, 71
- Parisi, M. C., Geisler, D., Carraro, G., et al. 2016, *AJ*, **152**, 58
- Parisi, M. C., Geisler, D., Clariá, J. J., et al. 2015, *AJ*, **149**, 154
- Parisi, M. C., Grocholski, A. J., Geisler, D., Sarajedini, A., & Clariá, J. J. 2009, *AJ*, **138**, 517
- Pawlowski, M. S., & Kroupa, P. 2014, *ApJ*, **790**, 74
- Perren, G. I., Piatti, A. E., & Vázquez, R. A. 2017, *A&A*, **602**, 89
- Piatti, A. E. 2011, *MNRAS*, **416L**, 89
- Piatti, A. E. 2011, *MNRAS*, **418L**, 69
- Piatti, A. E. 2012, *ApJL*, **756**, 32
- Piatti, A. E. 2014, *MNRAS*, **445**, 2302
- Piatti, A. E. 2017, *ApJL*, **834**, 14
- Piatti, A. E. 2018, *MNRAS*, **478**, 784
- Piatti, A. E., & Bica, E. 2012, *MNRAS*, **425**, 3085
- Piatti, A. E., Clariá, J. J., & Bica, E. 2011, *MNRAS*, **417**, 1559
- Piatti, A. E., de Grijs, R., Rubele, S., et al. 2015, *MNRAS*, **450**, 552
- Piatti, A. E., & Geisler, D. 2013, *AJ*, **145**, 17
- Piatti, A. E., Ivanov, V. D., Rubele, S., et al. 2016, *MNRAS*, **460**, 383
- Piatti, A. E., Santos, J. F. C., Jr., & Clariá, J. J. 2001, *MNRAS*, **325**, 792
- Piatti, A. E., Santos, J. F. C., Jr., Clariá, J. J., et al. 2005, *A&A*, **440**, 111
- Piatti, A. E., Sarajedini, A., Geisler, D., Clark, D., & Seguel, J. 2007, *MNRAS*, **377**, 300
- Piatti, A. E., Sarajedini, A., Geisler, D., Seguel, J., & Clark, D. 2005, *MNRAS*, **358**, 1215
- Pieres, A., Santiago, B. X., Drlica-Wagner, A., et al. 2017, *MNRAS*, **468**, 1349
- Pietrzynski, G., & Udalski, A. 1999, *AcA*, **49**, 157
- Rafelski, M., & Zaritsky, D. 2005, *AJ*, **129**, 2701
- Rich, R. M., da Costa, G. S., & Mould, J. R. 1984, *ApJ*, **286**, 517
- Rochau, B., Gouliermis, D. A., Brandner, W., Dolphin, A. E., & Henning, T. 2007, *ApJ*, **664**, 322
- Rubele, S., Girardi, L., Kerber, L. O., et al. 2015, *MNRAS*, **449**, 639
- Rubele, S., Kerber, L. O., & Girardi, L. 2010, *MNRAS*, **403**, 1156
- Sabbi, E., Sirianni, M., Nota, A., et al. 2007, *AJ*, **133**, 44
- Santiago, B. X., Elson, R. A. W., Sigurdsson, S., & Gilmore, G. F. 1998, *MNRAS*, **295**, 860
- Santos, J. F. C., Jr., Bica, E., Clariá, J. J., et al. 1995, *MNRAS*, **276**, 1155
- Schmalzl, M., Gouliermis, D. A., & Dolphin, A. E. 2008, *ApJ*, **681**, 290
- Schmeja, S., Gouliermis, D. A., & Klessen, R. S. 2009, *ApJ*, **694**, 367
- Seggewiss, W., & Richtler, T. 1989, in *Recent Developments of Magellanic Cloud Research*, ed. K. S. de Boer, F. Spite, & G. Stasińska (Meudon: Observatoire de Paris), 45
- Sitek, M., Szymański, M. K., Skowron, D. M., et al. 2016, *AcA*, **66**, 255
- Sitek, M., Szymański, M. K., Udalski, A., et al. 2017, *AcA*, **67**, 363
- Subramanian, S., Rubele, S., Sun, N.-C., et al. 2017, *MNRAS*, **467**, 2980
- Torrealba, G., Belokurov, V., & Koposov, S. E. 2019a, *MNRAS*, **484**, 2181
- Torrealba, G., Belokurov, V., Koposov, S. E., et al. 2019b, *MNRAS*, **488**, 2743
- Tsujimoto, T., & Bekki, K. 2009, *ApJL*, **700**, 69
- van den Bergh, S. 1981, *A&AS*, **46**, 79
- Westerlund, B. E. 1964, *MNRAS*, **127**, 429
- Zinn, R., & West, M. J. 1984, *ApJS*, **55**, 45
- Zivick, P., Kallivayalil, N., van der Marel, R. P., et al. 2018, *ApJ*, **864**, 55